

1 **Phase-specific stimulation of the human brain**

2 **with real-time measurement instead of prediction**

3 Robert Guggenberger\*, Julian-Samuel Gebühr, Marius Keute, Alireza Gharabaghi\*

4 Institute for Neuromodulation and Neurotechnology, University Hospital and

5 University of Tuebingen, Tuebingen, Germany

6

7 \*Correspondence

8 Institute for Neuromodulation and Neurotechnology, University Hospital and University of

9 Tuebingen, Otfried-Mueller-Str.45, 72076 Tuebingen, Germany. Email address:

10 [correspondence@robert-guggenberger.de](mailto:correspondence@robert-guggenberger.de); [alireza.gharabaghi@uni-tuebingen.de](mailto:alireza.gharabaghi@uni-tuebingen.de)

11

12

13

14

15

16

## 17 **Abstract**

18 Background: The responsiveness of the human brain to external input fluctuates. Timing the  
19 external perturbation with regard to the oscillatory brain state may improve the intended  
20 stimulation effects. However, current brain state-dependent interventions targeting phases of  
21 the oscillatory cycle need to apply prediction algorithms to compensate for latencies between  
22 measurement and stimulation, and are therefore imprecise.

23 Objective: We investigated the phase-specific precision of a novel non-predictive approach on  
24 the basis of integrated real-time measurement and brain stimulation.

25 Methods: Applying a simulation, we estimated the circular standard deviation (SD) to hit 2, 4,  
26 8, 16 or 32 equidistant phase bins of the oscillatory cycle with high precision. Furthermore, we  
27 used electroencephalography-triggered transcranial magnetic stimulation in healthy subjects  
28 to empirically determine the precision of hitting the targeted phase of the oscillatory cycle for  
29 10 different frequencies from 4Hz to 40Hz using our approach.

30 Results: The simulation revealed that SDs of less than  $17.6^\circ$ ,  $9.7^\circ$ ,  $5.1^\circ$ ,  $2.5^\circ$ , and  $1.3^\circ$  were  
31 necessary to precisely hit 2, 4, 8, 16, and 32 distinct phase bins of the oscillatory cycle. By  
32 completing measurement, signal-processing and stimulation with a round-time of 1ms, our  
33 empirical approach achieved SDs of  $0.4^\circ$  at 4Hz to  $4.3^\circ$  at 40Hz. This facilitates selective  
34 targeting of 32 phases (at 4Hz), 16 phases (at 8, 12, 16, 20, 24Hz) and 8 phases (at 28, 32,  
35 36, 40Hz), respectively.

36 Conclusion: Integrated real-time measurement and stimulation circumvents the need for  
37 prediction and results in more precise phase-specific brain stimulation than with state-of-the-  
38 art procedures.

39

40 **Keywords**

41 Phase-specific; phase-dependent; brain state-dependent; real-time; closed-loop; EEG-TMS

## 42 **Introduction**

43 The growing interest in brain state-informed interventions in neuroscience and therapy is  
44 driven by the motivation to achieve more predictable stimulation effects and neuroplastic  
45 changes. Specifically, EEG-triggered transcranial magnetic stimulation (TMS) has been  
46 applied to repetitively target sensorimotor rhythmic activity or oscillatory up- and down phases  
47 in order to induce increased corticospinal excitability in the human motor cortex, albeit with  
48 contradictory findings.<sup>1-3</sup>

49 To identify the impact of stimulation timing on fluctuations of motor-evoked potential (MEP)  
50 amplitudes, the pre-TMS power and phase at the site of stimulation have been investigated  
51 with post-hoc analysis.<sup>4</sup> Specifically, a 40-70% MEP amplitude increase was detected across  
52 different beta power levels, thereby implying a certain robustness against imprecise  
53 stimulation timing. By contrast, the phase-modulation was critically dependent on precisely  
54 timing the stimuli to specific phases of the oscillatory cycle. Importantly, when this phase  
55 specificity was achieved, a MEP increase of 180% could be attained.<sup>4</sup>

56 Different methods are currently being applied to predict the oscillatory phase for state-  
57 informed stimulation: Autoregressive (AR) model-based approaches;<sup>5</sup> Kalman filter-based AR  
58 approaches for long-term predictions (> 100 ms);<sup>6</sup> least mean square (LMS)-based AR  
59 approaches for adaptive predictions with recurrent updates;<sup>7</sup> approaches that utilize pre-  
60 learned features;<sup>8</sup> and machine learning-based approaches on the basis of training data.<sup>9</sup>  
61 Importantly, these approaches often apply their phase predictions to lower frequency  
62 oscillations, since these have inherently less strict demand for temporal precision than higher  
63 frequency oscillations. The higher the frequency, the more challenging the task of targeting a  
64 specific phase bin, since the round-trip time needs to be less than the width of the bin for the

65 target frequency. This challenge becomes particularly apparent when more precise phase  
66 targeting than hitting two opposite phases (e.g., peak vs. trough) in the alpha band is  
67 necessary to achieve the intended stimulation effect, e.g., by hitting a non-overlapping phase  
68 bin of  $1/8$  of the oscillatory beta cycle.<sup>4</sup>

69 In the present study, we aimed to address this question in two ways: First, we estimated the  
70 circular SD required to hit 2, 4, 8, 16 and 32 equidistant and non-overlapping phase bins of  
71 the oscillatory cycle with high precision. Second, we investigated the phase-specific precision  
72 of a non-predictive approach on real data, i.e., with EEG-triggered TMS using a novel device  
73 based on embedded real-time measurement and stimulation. We hypothesized that this novel  
74 online stimulation approach would allow selective phase-targeting across different – also  
75 higher – frequency bands with the necessary precision.

76

## 77 **Methods**

### 78 *Simulation*

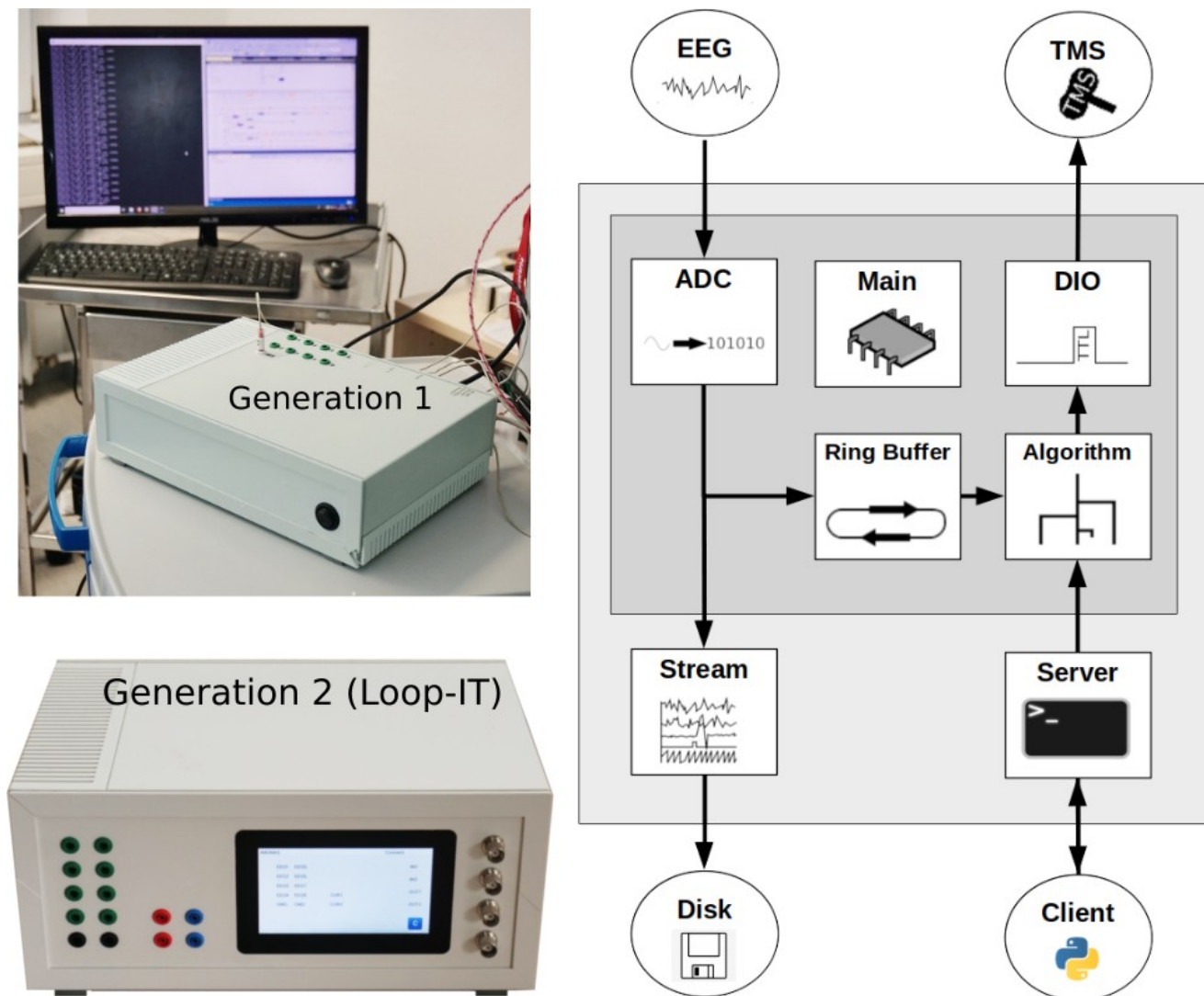
79 We estimated the circular SD required to target equidistant and non-overlapping phase bins  
80 of the oscillatory cycle with an error rate of less than 1 in 10 000. Specifically, we drew 100  
81 000 draws from a von Mises distribution with varying  $k$ . This resulted in 500 simulated  
82 datasets (with  $k$  from 100 to 1010). To be comparable to other studies on this topic, we  
83 calculated the circular SD for each simulated dataset. This resulted in SDs ranging from  
84  $0.0005^\circ$  to  $72.8^\circ$ . We investigated 2, 4, 8, 16 and 32 non-overlapping phase bins. The width of  
85 the phase bins was therefore changing with the number of bins. For example, the width was  
86  $180^\circ$  in the case of 2 phase bins and  $11.25^\circ$  in the case of 32 phase bins. Finally, we  
87 calculated for each simulated dataset, how often a sample would land outside the width of a  
88 phase bin. For each number of phase bin, we also calculated the SD resulting in an error rate  
89 of less than 1 in 10 000. We selected this strict threshold to achieve high precision, also when  
90 considering large studies with many participants and multiple sessions.

### 91 *Real-time measurement and stimulation device*

92 The novel real-time measurement and stimulation device (rtMSD) implemented and  
93 investigated here enables us to measure electrophysiological signals, analyze them  
94 instantaneously, and return a digital output for triggering external stimulation devices. The  
95 device is comprised of separate modules, each with its own defined functionality. The latest  
96 version of the rtMSD contains four essential elements in a common housing. The first element  
97 is the control chip which ensures real-time communication between all elements. It also drives  
98 a set of LEDs to indicate status and functionality of the device and its modules. The second  
99 element is a system on a chip (SoC), running a Linux-based operating system. In this

100 environment, custom-written software supports sending data and receiving commands to and  
101 from external computers, and performing the signal processing and phase detection in real  
102 time. The third element is an analog-to-digital converter which allows the digitization of up to 8  
103 channels of electrophysiological measurements. The last element is a digital input/output  
104 connected to two BNC adapters providing TTL input and output and triggering external  
105 devices. The first generation of the device used a separate PC instead of the SoC, whereas  
106 the current version is completely embedded (see figure 1) and was manufactured in  
107 collaboration with neuroConn (Loop-IT, Ilmenau, Germany).

108



109 **Figure 1: Integrated real-time measurement and stimulation device.** *The left two images*  
110 *show the first and second generation of the device, and the right diagram shows the internal*  
111 *architecture of both generations. The dark gray box shows the real-time components, the light*  
112 *gray box shows the components with a permissible jitter, and the circles outside the boxes*  
113 *indicate external elements. The EEG is measured, converted and stored in a ringbuffer,*  
114 *which is used by the algorithm to trigger stimulation (e.g., TMS) via a digital input/output*  
115 *interface. The main module realizes real-time performance by cyclic execution and*  
116 *information transfer between the modules. Parameters of the trigger algorithm are shared*  
117 *with a server, which can communicate with an external client for reading and writing the*  
118 *parameters. Raw data and derived measures are streamed online via LabStreamingLayer*  
119 *and can be recorded on an external PC.*

120

121 *From EEG recording to TMS pulse application*

122 Algorithms for signal processing and analysis as well as phase detection and triggering can  
123 be programmed using a high-level language (EN 61131-3 or C/C++) and run on the SoC of  
124 the rtMSD directly. The following approach was implemented to evaluate the phase precision  
125 of the device. EEG was recorded in a bipolar montage, with two electrodes placed 1 cm  
126 anterior and posterior of C3 with the ground electrode on the forehead, and sampled at 1 kHz  
127 at a resolution of 24 bit. The bipolar signal was stored in a ring buffer of 500 ms length,  
128 implemented as a circular buffer of 500 doubles in memory for improved speed. The window  
129 size was defined on the basis of our experience from previous experiments.<sup>1,10</sup> A discrete  
130 Fourier transform for a specific frequency was performed every millisecond with the Görtzel  
131 algorithm.<sup>11</sup> Taking the buffer width of 500ms into account, this provided a frequency  
132 resolution of 2 Hz and a phase estimate for each sample. The trigger algorithm considers the



133 current phase and compares it with the phase of the last sample. When the circular arc  
134 between the last and the current phase estimate includes the target phase, thereby  
135 ascertaining that the target phase has been passed, a trigger signal is delivered. Additionally,  
136 the raw EEG data and the calculated phase and trigger channel are streamed together using  
137 the LabStreamingLayer. This makes it possible to collect the data on an external PC, where it  
138 is then stored on a disk.

### 139 *Empirical evaluation*

140 To evaluate the feasibility of this device in practical applications, the 5 V trigger signal was  
141 routed via BNC to a TMS device (MagPro X100, MagVenture, Denmark). Since triggering an  
142 external device can induce additional latency and inherent jitter, we evaluated the delay of the  
143 TMS device by driving it repetitively with a signal generator and measuring the stimulation  
144 delay with an oscilloscope. This experiment suggested that the TMS device added ~65  $\mu$ s  
145 delay, which can be considered negligible for most practical applications.

146 We evaluated the performance of the rtMSD in 4 right-handed participants (1 female, age M =  
147 23.75, SD = 1.09) who gave their written informed consent prior to participation. The study  
148 protocol conformed to the Declaration of Helsinki and was approved by the Ethical Committee  
149 of the medical faculty of the University of Tübingen. The study followed the current safety  
150 guidelines for application of TMS,<sup>12</sup> and none of the participants reported side effects.

151 To study the phase precision of the device over a wide range of frequencies, we investigated  
152 10 different target frequencies (4, 8, 12, 16, 20, 24, 28, 32, 36 and 40 Hz) in randomized  
153 order at the target phase of 0°. Stimuli were triggered with an interstimulus interval (ISI) of  
154 3.5-4.5s. We used a jitter of  $\pm$  0.5 seconds to reduce anticipation effects. We applied TMS at  
155 120 % resting motor threshold (RMT) to the motor hot spot of the left hemisphere with a pulse

156 width of 280  $\mu$ s, using biphasic pulses that are considered more effective in inducing MEPs  
157 than monophasic pulses.<sup>13</sup> Due to technical artifacts, 95 trials (11.88 %) were rejected,  
158 resulting in overall 705 pulses in the four participants, with 51 to 69 trials per target frequency.

159

### 160 *Performance measures*

161 Bearing in mind that our algorithm triggers only when the target phase has been passed, we  
162 expected a linear increase in the phase delay with increasing frequency and compared it to  
163 the measured phase delay (see below).

164 Furthermore, we measured the precision of our stimulation by estimating the circular standard  
165 deviation (SD). This entailed cutting 500 ms segments from the recorded signal that ended  
166 immediately prior to each trigger and filtering it with a single-order two-way Butterworth filter  
167 using a passband of  $\pm 1$  Hz around the target frequency. To reduce edge artifacts, the  
168 segment was wrap-padded with 1000 samples on each side before filtering. The resulting  
169 filtered segments were z-transformed to prevent bias between trials due to unequal signal  
170 power. Finally, we averaged all segments per target frequency and calculated the resulting  
171 confidence interval at each sample.

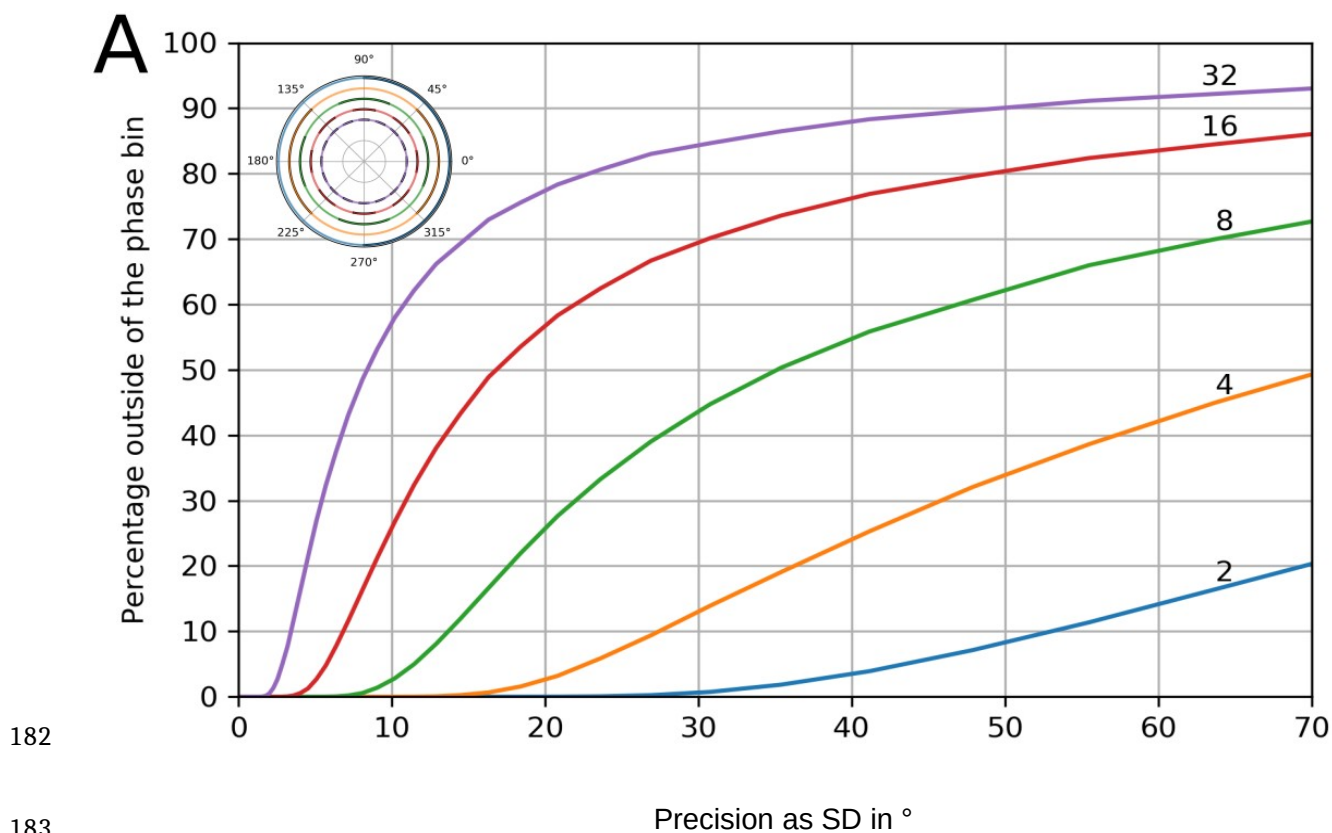
### 172 *Software Packages*

173 Offline digital processing and statistical analysis were performed using NumPy 1.20.3 and  
174 SciPy 1.5.2 on Python 3.7.6 on Linux Mint 20. Additionally, we used pyCircStat 0.0.2 and  
175 Statsmodels 0.12.0 and Matplotlib 3.1.3 for visualization.

176

177 **Results**

178 The simulation revealed that circular SDs of less than 17.6°, 9.7°, 5.1°, 2.5°, and 1.3° are  
179 necessary to hit a specific phase of the oscillatory cycle divided into 2, 4, 8, 16, and 32 non-  
180 overlapping phase bins with sufficient precision (i.e., an error rate of smaller than 1/10.000)  
181 (fig.2).



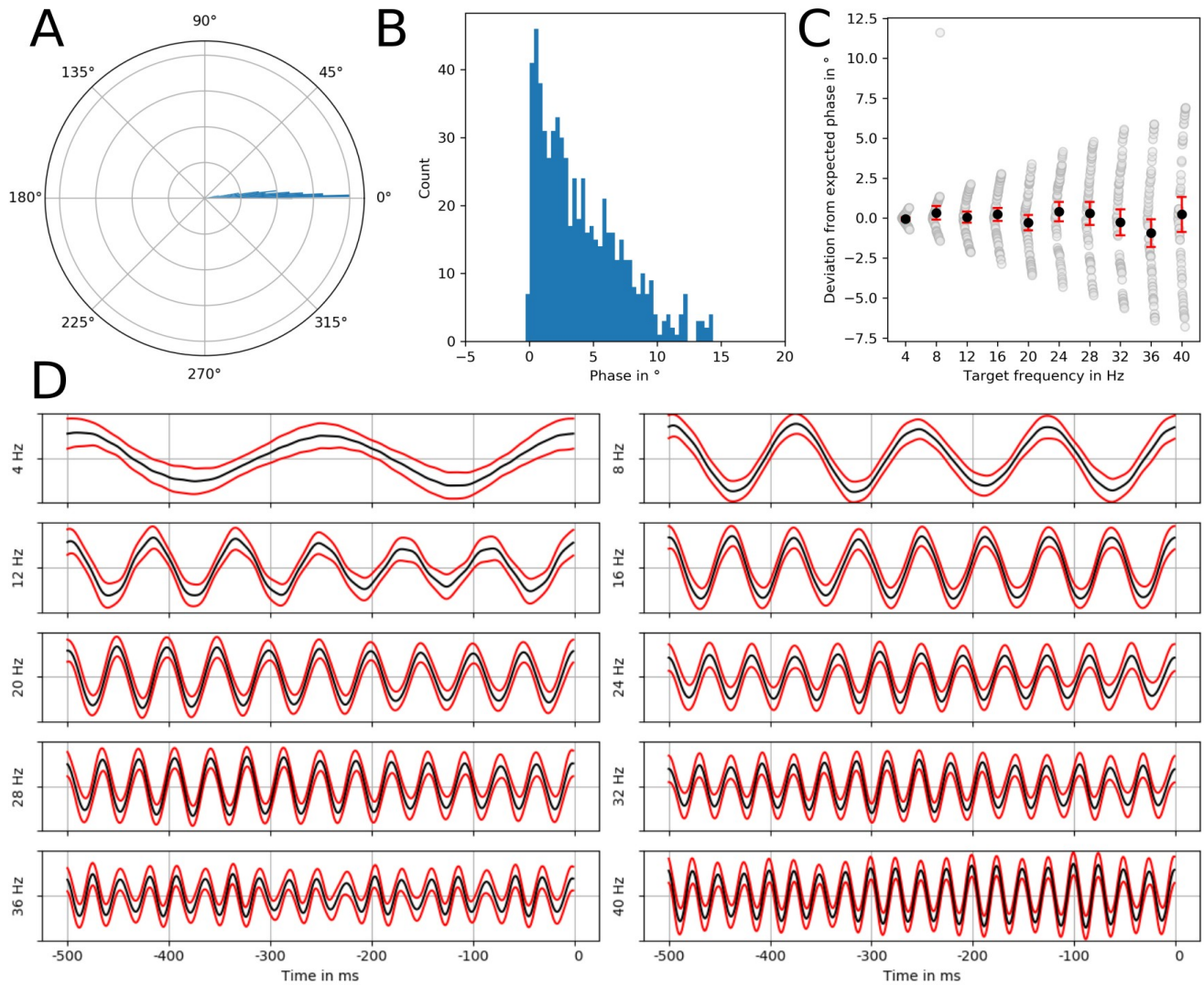
184 **Figure 2: Simulated precision of phase-dependent modulation.** *The performance curves*  
185 *are plotted with the x-axis showing the circular standard deviance in degrees, indicating the*  
186 *phase precision. The y-axis shows how many samples lie outside of the respective phase bin*  
187 *for a given width on the basis of the number of bins. Each colored line represents a different*  
188 *number of non-overlapping equidistant phase bins, with the bin number ranging from 2 to 32.*

189 *The inlet in the upper left corner visualizes the number of phase bins for different samplings*  
190 *(from 2 to 32) on the unit circle with dark and light arcs.*

191 The empirical approach completed the measurement, signal-processing and stimulation with  
192 a round-trip time of 1 ms, which led to short phase delays for all frequencies between 4 and  
193 40 Hz (figure 3A). Across all frequencies, the spread exhibited a strongly left-skewed  
194 distribution (figure 3B). This observation is in line with the expected increase in phase delay  
195 as frequency increased, i.e., shorter length of the respective oscillatory cycle. For each  
196 frequency investigated, the measured phase was invariably very close to the expected phase  
197 delay (see figure 3C), thus allowing for a systemic lag-correction. The grand average of the  
198 pre-stimulation segments showed that the bandpass-filtered signal exhibited a sinusoidal  
199 modulation, with the stimulation occurring at the peak of the oscillation across frequencies, as  
200 expected when triggering at 0° (see figure 3D).

201 Importantly, our approach achieved very low SDs of 0.4° at 4 Hz to 4.3° at 40 Hz from the  
202 targeted phases (table 1). This high precision enabled us to selectively target 32 phases (at 4  
203 Hz), 16 phases (at 8, 12, 16, 20, 24 Hz) and 8 phases (at 28, 32, 36, 40 Hz), respectively,  
204 when considering the findings of the simulation.

205



206

207 **Figure 3: Visualized phase delay and precision (confidence interval) of the integrated**  
208 **real-time measure and stimulation device.** *The upper row shows the phase delay for the*  
209 *targeted frequencies. (A) The density estimates are given in polar coordinates and arbitrary*  
210 *units (A) and as a count histogram (B). A wheat scatter plot (C) shows the distributed (gray)*  
211 *and average (black) deviance from the expected phase, and the red lines indicating the 95%*  
212 *confidence interval. (D) Band-pass filtered grand average EEG data (black) 500ms before the*  
213 *TMS pulse and the 95% confidence interval (red).*

214

Target Frequency	Expected Phase Delay	Measured Phase Delay	Standard deviation	N
4 Hz	0.72°	0.67°	0.39°	51
8 Hz	1.44°	1.77°	1.67°	61
12 Hz	2.16°	2.22°	1.38°	65
16 Hz	2.88°	3.12°	1.68°	67
20 Hz	3.60°	3.32°	2.00°	69
24 Hz	4.32°	4.73°	2.46°	65
28 Hz	5.04°	5.33°	2.90°	65
32 Hz	5.76°	5.50°	3.37°	67
36 Hz	6.48°	5.54°	3.56°	68
40 Hz	7.20°	7.43°	4.30°	61

215

216 **Table 1: Expected and measured phase delay and standard deviation of the integrated**  
217 **real-time measure and stimulation device for different target frequencies.** *The overall*  
218 *accuracy consists of the measured phase delay and the standard deviation (precision). With*  
219 *a defined system latency (i.e., measurement, signal-processing and stimulation with a round-*  
220 *time of 1 ms), the expected phase delay increases with increasing target frequency, i.e.,*  
221 *shorter length of the respective oscillatory cycle. Since the measured phase delay matched*  
222 *the expected phase delay, a systemic lag-correction of this predictable system delay is*  
223 *possible. The standard deviation (precision), however, is related to the system's jitter and/or*  
224 *non-stationarity of the target frequency, and is therefore unpredictable. This precision is*  
225 *essential to specifically target the intended phase bin.*

## 226 Discussion

227 We investigated the phase-specific precision of state-dependent neuromodulation on the  
228 basis of integrated real-time measurement and brain stimulation. By completing  
229 measurement, signal-processing and stimulation with a round-time of 1 ms, this novel non-  
230 predictive approach achieved high empirical precision in the real-life scenario of EEG-  
231 triggered TMS. Specifically, the standard deviations across ten different frequencies were  $0.4^\circ$   
232 at 4 Hz to  $4.3^\circ$  at 40 Hz. According to our simulations, this precision would facilitate the  
233 selective targeting of 8 distinct phases in all investigated frequencies up to 40 Hz. This  
234 precision would be sufficient to achieve the necessary phase specificity of TMS to maximize  
235 MEP increases in accordance with previous post-hoc estimations.<sup>4</sup>

236 By contrast, previous autoregressive (AR) model-based approaches using pre-stimulus  
237 estimation of the brain state for EEG-triggered TMS do not achieve such high precision as  
238 they require the application of prediction algorithms to compensate for latencies between  
239 measurement and stimulation. Accordingly, previous studies applied EEG-triggered TMS to  
240 investigate research questions that could be addressed with less temporal precision; e.g., by  
241 applying EEG-triggered TMS on the basis of (a) high and low oscillatory power levels in the  
242 beta band (16-22 Hz) and (b) positive and negative peaks of the slow ( $< 1$ Hz) or alpha (8-12  
243 Hz) oscillatory cycle to study instantaneous and lasting MEP amplitude changes: Specifically,  
244 brain state-dependent TMS, when controlled by volitionally modulated low sensorimotor beta  
245 power levels, induced a robust MEP amplitude increase.<sup>1</sup> By contrast, when the very same  
246 stimulation pattern was applied independent of the brain state, a decrease in corticospinal  
247 excitability ensued. When TMS was applied during sleep, targeting depolarized vs.  
248 hyperpolarized phases of slow oscillations was associated with an increase in instantaneous  
249 MEP amplitudes.<sup>14</sup> During wakefulness, sensorimotor alpha oscillations at rest were used to

250 trigger TMS, targeting the negative vs. positive peak of the oscillatory cycle and thus leading  
251 to a lasting increase vs. no change in MEP amplitude in a preselected group of participants  
252 with high sensorimotor alpha power.<sup>2</sup> However, this finding was not replicated when the same  
253 approach was applied in non-selected individuals.<sup>3</sup> Importantly, these online approaches hit  
254 the targeted negative/positive peaks of the alpha cycle with standard deviations of  $55^\circ/53^\circ$ <sup>2</sup>  
255 and  $48^\circ/52^\circ$ .<sup>3</sup>

256 According to the simulation of this study (figure 2), a considerable number of stimuli would be  
257 outside the target phase bin when imprecise stimulation with a SD of  $\sim 50^\circ$  is applied with  
258 previous approaches. Specifically,  $>30\%$  of stimuli would be off-target for a phase resolution  
259 of 4 bins, which is necessary to estimate sinusoidal modulation. Furthermore,  $>60\%$  of stimuli  
260 would be off-target for a phase resolution of 8 bins, which has been shown to be necessary to  
261 capture phase-dependent effects of corticospinal excitability in the oscillatory beta-band.<sup>4</sup>

262 The inconsistencies of these previous observations may therefore be related to different  
263 factors: On the one hand, the relative imprecision of hitting the targeted phase of the alpha  
264 cycle may have prevented more robust and reproducible findings with regard to TMS induced  
265 plastic changes. On the other hand, the intrinsic targeting error of current approaches is  
266 amplified when higher frequency bands are investigated, and thus limits studying the phase-  
267 dependency of frequencies that may shape the timing of voluntary movements and  
268 determined corticospinal excitability in earlier offline analyses.<sup>15-18</sup>

269 Moreover, the interaction between oscillatory phase and power may influence corticospinal  
270 excitability to an extent unexplained by phase or power alone.<sup>19</sup> Also, resolving current  
271 contradictions of phase dependency in different frequencies<sup>15,20</sup> may necessitate high-  
272 resolution sampling along the oscillatory cycle (e.g., by comparing 8 equidistant phases in  
273 each investigated frequency) to allow for robust modeling of input-output relationships.<sup>21</sup>



274 Furthermore, minor differences in the methodological choices may critically affect the  
275 sensitivity to detect the complex relationship between oscillatory activity and corticospinal  
276 excitability<sup>22</sup> and even lead to erroneous phase estimations.<sup>23</sup>

#### 277 Limitations and perspectives

278 The technological feasibility of highly precise phase-specific stimulation does not per se lead  
279 to the intended stimulation effects and desired outcome. Before translating this approach to  
280 broad scientific and clinical application, relevant open questions need to be addressed:  
281 Although hitting the intended phase precisely may result in reduced variability of  
282 instantaneous stimulation effects, as demonstrated in previous post-hoc analyses,<sup>17</sup> these  
283 less variable stimulation effects do not necessarily lead to cumulative stimulation effects and  
284 plastic changes after repetitive application. Moreover, it needs to be clarified how consistent  
285 phase-dependent stimulation effects are in cross-validation experiments, e.g., with out-of-  
286 sample evaluation within one session, across different sessions and days, and between  
287 individuals with regard to the optimal frequency and phase bin of the oscillatory cycle.<sup>21</sup>  
288 Furthermore, stimulation pulses may also be timed to the most sensitive phase with novel  
289 computation methods that are more precise and faster than previous prediction approaches  
290 by modeling a linear oscillator and recomputing the phase of this virtual oscillator into the  
291 analyzed signal.<sup>24,25</sup> Notably, the sinusoidal nature of cortical oscillations, and whether they  
292 might be better characterized by their non-sinusoidality, is currently a matter of some  
293 debate.<sup>26,27</sup> However, such open questions may now be addressed with this novel non-  
294 predictive stimulation approach.

295 In conclusion, integrated real-time measurement and brain stimulation circumvented the need  
296 for prediction and allowed state-informed stimulation with high precision. The applied  
297 approach of EEG-triggered TMS resulted in selective targeting of 8 distinct phases in the

298 investigated frequencies of up to 40 Hz, thereby attaining the necessary specificity to  
299 maximize instantaneous stimulation effects. Future studies need to clarify whether this will  
300 also lead to increased cumulative stimulation effects and plastic changes, and whether  
301 phase-specific stimulation may influence brain disorders that are characterized by aberrant  
302 neural oscillations.<sup>28-31</sup>

303

304 **Authorship contribution statement**

305 Robert Guggenberger: Conceptualization, Methodology, Software, Data curation, Formal  
306 analysis, Writing - original draft, Visualization. Julian-Samuel Gebühr: Methodology, Software,  
307 Investigation, Data curation, Writing - review & editing. Marius Keute: Methodology, Software,  
308 Writing - review & editing. Alireza Gharabaghi: Conceptualization, Writing - original draft,  
309 Supervision, Project administration, Funding acquisition.

310

311 **Declaration of Competing Interest**

312 The authors declare no conflict of interests.

313

314 **Acknowledgments**

315 This work was supported by the German Federal Ministry of Education and Research  
316 [BMBF16SV8174, INERLINC]. We acknowledge support from the Open Access Publishing  
317 Fund of the University of Tuebingen.

318

319 **Data availability statement**

320 The data that support the findings of this study are available for researchers from the first  
321 author upon reasonable request.

## 322 **References**

1. Kraus D, Naros G, Bauer R, Khademi F, Leão MT, Ziemann U, Gharabaghi A. (2016) Brain State-Dependent Transcranial Magnetic Closed-Loop Stimulation Controlled by Sensorimotor Desynchronization Induces Robust Increase of Corticospinal Excitability. *Brain Stimul.* 9:15-424.
2. Zrenner C, Desideri D, Belardinelli P, Ziemann U (2018) Real-time EEG-defined excitability states determine efficacy of TMS-induced plasticity in human motor cortex. *Brain Stimul* 11: 374-389.
3. Madsen KH, Karabanov AN, Krohne LG, Safeldt MG, Tomasevic L, Siebner HR (2019) No trace of phase: Corticomotor excitability is not tuned by phase of pericentral mu-rhythm. *Brain Stimul* 12:1261–1270.
4. Khademi F, Royter V, Gharabaghi A (2019) State-dependent brain stimulation: Power or phase? *Brain Stimul* 12:296-299.
5. Chen LL, Madhavan R, Rapoport BI, Anderson WS (2013) Real-time brain oscillation detection and phase-locked stimulation using autoregressive spectral estimation and time-series forward prediction. *IEEE Trans Biomed Eng.* 60:753-62.
6. Onojima T, Kitajo K. (2021) A state-informed stimulation approach with real-time estimation of the instantaneous phase of neural oscillations by a Kalman filter. *J Neural Eng.* 9;18(6).

7. Shakeel A, Onojima T, Tanaka T, Kitajo K (2021) Real-Time Implementation of EEG Oscillatory Phase-Informed Visual Stimulation Using a Least Mean Square-Based AR Model. *J Pers Med.* 11;11(1):38
8. Shirinpour, S., Alekseichuk, I., Mantell, K., & Opitz, A. (2020). Experimental evaluation of methods for real-time EEG phase-specific transcranial magnetic stimulation. *Journal of neural engineering*, 17(4), 046002.
9. McIntosh JR, Sajda P (2020) Estimation of phase in EEG rhythms for real-time applications. *J Neural Eng.* 2020 Jun 2;17(3):034002.
10. Raco V, Bauer R, Tharsan S, Gharabaghi A (2016) Combining TMS and tACS for Closed-Loop Phase-Dependent Modulation of Corticospinal Excitability: A Feasibility Study. *Front Cell Neurosci* 10:143.
11. Sorensen HV, Burrus CS, Jones DL (1988) A new efficient algorithm for computing a few DFT points. In: 1988., IEEE International Symposium on Circuits and Systems, pp 1915–1918.
12. Rossi S, Antal A, Bestmann S, Bikson M, et al. (2021) Safety and recommendations for TMS use in healthy subjects and patient populations, with updates on training, ethical and regulatory issues: Expert Guidelines. *Clin Neurophysiol.* 132:269-306.
13. Terao Y, Ugawa Y (2002) Basic Mechanisms of TMS: *J Clin Neurophysiol* 19:322–343.
14. Bergmann TO, Mölle M, Schmidt MA, Lindner C, Marshall L, Born J, Siebner HR (2012) EEG-guided transcranial magnetic stimulation reveals rapid shifts in motor cortical excitability during the human sleep slow oscillation. *J Neurosci* 32:243–253.

15. Khademi F, Royter V, Gharabaghi A (2018) Distinct Beta-band Oscillatory Circuits Underlie Corticospinal Gain Modulation. *Cereb Cortex* 28:1502–1515.
16. Naros G, Lehnertz T, Leão MT, Ziemann U, Gharabaghi A (2020) Brain State-dependent Gain Modulation of Corticospinal Output in the Active Motor System. *Cereb Cortex*. 10; 30:371-381
17. Torrecillos, F., Falato, E., Pogosyan, A., West, T., Lazzaro, V. D., & Brown, P (2020). Motor Cortex Inputs at the Optimum Phase of Beta Cortical Oscillations Undergo More Rapid and Less Variable Corticospinal Propagation. *J Neurosci* 40, 369–381.
18. Hussain SJ, Vollmer MK, Iturrate I, Quentin R. (2022) Voluntary Motor Command Release Coincides with Restricted Sensorimotor Beta Rhythm Phases. *J Neurosci*. 20; 42:5771-5781.
19. Hussain, S. J., Claudino, L., Bönstrup, M., Norato, G., Cruciani, G., Thompson, R., ... & Cohen, L. G. (2019). Sensorimotor oscillatory phase–power interaction gates resting human corticospinal output. *Cerebral Cortex*, 29(9), 3766-3777.
20. Wischnewski M, Haigh ZJ, Shirinpour S, Alekseichuk I, Opitz A. (2022) The phase of sensorimotor mu and beta oscillations has the opposite effect on corticospinal excitability. *Brain Stimul*. 15:1093-1100.
21. Keute M, Gebühr JS, Guggenberger R, Trunk BH, Gharabaghi A (2022) Phase-specific stimulation reveals consistent sinusoidal modulation of human corticospinal excitability along the oscillatory beta cycle. (under review)

22. Karabanov AN, Madsen KH, Krohne LG, Siebner HR. (2021) Does pericentral mu-rhythm "power" corticomotor excitability? A matter of EEG perspective. *Brain Stimul.*14:713-722.
23. Khademi F, Royter V, Ziegler L, Gharabaghi A (2022) Resolving equivocal gain modulation of corticospinal excitability. (under review)
24. Rosenblum, M. (2020). Controlling collective synchrony in oscillatory ensembles by precisely timed pulses. *Chaos: An Interdisciplinary Journal of Nonlinear Science*, 30(9), 093131.
25. Busch JL, Feldmann LK, Kühn AA, Rosenblum M. (2022) Real-time phase and amplitude estimation of neurophysiological signals exploiting a non-resonant oscillator. *Exp Neurol.* 347:113869.
26. Cole SR, Voytek B (2017) Brain Oscillations and the Importance of Waveform Shape. *Trends Cogn Sci* 21:137–149.
27. Schaworonkow N, Nikulin VV (2019) Spatial neuronal synchronization and the waveform of oscillations: Implications for EEG and MEG Battaglia FP, ed. *PLOS Comput Biol* 15: e10070551:
28. Azodi-Avval, R., & Gharabaghi, A. (2015). Phase-dependent modulation as a novel approach for therapeutic brain stimulation. *Frontiers in computational neuroscience*, 9, 26.
29. Cagnan H, Pedrosa D, Little S, Pogosyan A, ... & Brown P. (2017) Stimulating at the right time: phase-specific deep brain stimulation. *Brain.*140:132-145.

30. Holt AB, Kormann E, Gulberti A, Pötter-Nerger M, ... & Sharott A. (2019) Phase-Dependent Suppression of Beta Oscillations in Parkinson's Disease Patients. *J Neurosci.* 6; 39:1119-1134.
31. McNamara, C. G., Rothwell, M., & Sharott, A. (2020). Phase-dependent closed-loop modulation of neural oscillations in vivo. *BioRxiv*.